

Thermodynamic Characteristics of the Hydrogen Sulfide Sorption Process by Ferromanganese Materials

Olga V. Cheremisina, Maria A. Ponomareva,* Victor A. Bolotov, Artyom S. Osipov, and Alexandr V. Sitko



Cite This: *ACS Omega* 2022, 7, 3007–3015

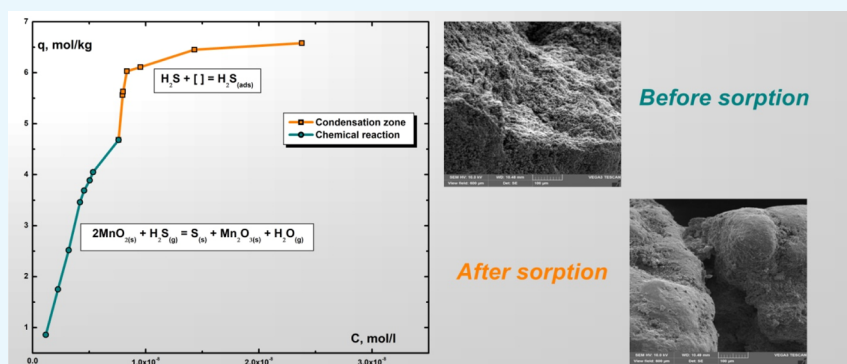


Read Online

ACCESS |

Metrics & More

Article Recommendations



ABSTRACT: The work analyzes hydrogen sulfide sorption from model gas mixtures containing H_2S from 1.25×10^{-3} to 1.28×10^{-4} mol/L under static conditions at temperatures 253 and 298 K on the raw manganese ore of the Ulu-Telyak deposit (Bashkortostan, Russia), manganese(IV) oxide, and manganese(IV) and iron(III) oxide mixtures. The thermodynamic models for calculating the equilibrium constants and Gibbs energy changes were analyzed. The sorption isotherms were described by the Langmuir, Freundlich, Temkin, and Dubinin–Radushkevich models. The value of enthalpy $\Delta H_{(253-298)}^0$ of hydrogen sorption on the ore was -68.98 ± 3.45 kJ/mol and those on model mixtures $\text{Mn}_4 + \text{Fe}_2\text{O}_3$ and MnO_4 were ± 12.20 kJ/mol and -103.826 ± 5.19 kJ/mol, respectively, and the entropies of the hydrogen sulfide sorption process on three manganese materials at 253 K were calculated. The limiting capacity values of manganese materials at 253 and 298 K were obtained. The morphological analysis of the ore samples, $\text{Mn}_4 + \text{Fe}_2\text{O}_3$, and MnO_4 , before and after hydrogen sulfide sorption, was carried out at 253 K. The obtained thermodynamic parameters determine the advantage of using the raw manganese ore over pure oxides, which characterizes its effective practical application in the desulfurization process.

INTRODUCTION

Technological processes associated with the processing of minerals, in particular, apatite-nepheline raw materials, as well as metallurgical and chemical production, lead to the formation of large amounts of waste, which is an environmental problem of mineral complexes. One of the significant problems is the emission of process gases into the atmosphere containing toxic substances, including sulfur-containing compounds.^{1–6}

The problem of atmospheric pollution in large city areas, located close to metallurgical and oil refining enterprises and enrichment factories, has recently reached critical levels.^{7–9}

The main ways of technological gas purification from polluting components are mechanical purification and physicochemical methods, which are most often used with various mineral sorbents based on manganese materials,^{10,11} zeolites,¹² and active coals¹³ of different origins, sorbents based on metal oxides,^{14,15} and other synthetic materials.^{16,17} The process of

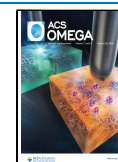
sorption and purification of gases from sulfur-containing and other components is often accompanied by the conversion process, as in the work,¹⁸ in which the study of sorption of hydrogen sulfide on CaCO_3 was carried out, as a result of which conversion of $\text{H}_2\text{S} \rightarrow \text{CaS}$ was observed.

When studying the sorption processes of toxic pollutant components, the determination of thermodynamic parameters, such as the equilibrium constant value, Gibbs energy changes, enthalpy, and entropy, allows predicting the processes of

Received: October 28, 2021

Accepted: December 31, 2021

Published: January 11, 2022



emission gas purification and conducting technological calculations.^{19–21}

The authors of the work²² propose using eggshells—waste products of the food industry with a high content of calcium to remove sulfur dioxide (SO₂) and hydrogen sulfide (H₂S). Eggshells calcined at 900 °C showed the best adsorption capacity for both SO₂ (3.53 mg/g) and H₂S (2.62 mg/g). Under 40% humidity conditions in the initial gas, the adsorption capacity improved significantly to about 11.68 and 7.96 mg/g, respectively. The authors established the chemisorption mechanism of gas sorption.

The aim of the work²³ was to determine the characteristics of a composite based on α -FeOOH for the removal of hydrogen sulfide in gas streams at room temperature. α -FeOOH was obtained using a solution of FeCl₃ and N₄HCO₃ (to control the pH) and applied to activated carbon powder to avoid agglomeration during composite fabrication. The experimental results show that activated carbon powder is effective as a composite base preventing the agglomeration of α -FeOOH sludge particles and providing a high adsorption capacity of the material of 0.171 g/g compared to pure α -FeOOH of 0.046 g/g.

By the coprecipitation of manganese nitrate and aluminum nitrate, a series of sorbents with different contents of manganese were obtained, as proposed by the authors of the work²⁴ for the removal of H₂S from gaseous media at a temperature of 850 °C. It was found that the capacity concerning sulfur increases linearly with increasing manganese content. The authors performed experiments on sulfidation and regeneration and found that the sorbents are stable over five cycles. Material regeneration was carried out using oxygen, sulfur dioxide, and steam. The sorbents under study can be completely regenerated by steam; the regeneration product in this case is H₂S.

The authors of the work²⁵ obtained nanocomposites based on copper, zinc, and nickel impregnated on an activated carbon surface (Cu–Zn–Ni-NPs–AC) and cobalt and nickel nanoparticles impregnated on γ -Al₂O₃ (Ni–Co-NPs– γ Al₂O₃). These materials are used to remove hydrogen sulfide from natural gas. The optimal parameter values were 0.3 g of the adsorbent, a flow rate of 0.15 L/min, and a temperature of 15 °C. Carrying out the process in the above-stated conditions allowed reaching the maximum hydrogen sulfide removal: 94 and 91.6% for Cu–Zn–Ni-NPs–AC and Ni–Co-NPs– γ Al₂O₃, respectively. Thermodynamic calculations showed that the Gibbs energy of the adsorption process for each of the materials is negative; the experimental data of equilibrium adsorption for both adsorbents can be described by the Langmuir model with the highest correlation coefficients.

Coconut shell-activated carbon (ACS-1) was used as a sorbent for the simultaneous removal of H₂S and CO₂ from the flue gases of the Claus process by the authors of the work.²⁶ It was found that gas concentrations can be reduced to less than 10 mg/m³ with the proposed adsorbent, and the measured sulfur capacity of the material was 64.27 mg/g. The main active centers for the adsorption of hydrogen sulfide and sulfur dioxide were micropores of size about 0.5 nm, while mesopores showed little desulfurization activity. The desulfurization process was carried out by both physical adsorption and chemical adsorption.

The primary adsorption of H₂S and SO₂ on ACS-1 is physical adsorption, followed by the partial oxidation of the parent components by oxygen adsorbed on ACS-1 to elemental sulfur and sulfate, respectively. At the same time, the Claus reaction between H₂S and SO₂ takes place. In addition, the ACS-1 sorbent can be completely regenerated using water vapor at 450

°C with the adsorption capacity retained for five adsorption–regeneration cycles.

The authors of the work²⁷ suggested using the adsorbent MSM-41, modified with amino groups by the impregnation method for the removal of hydrogen sulfide from natural gas. At 45 °C, the capacity concerning sulfur was 134.38 mg/g and the degree of desulfurization reached 54.19%. The experimental adsorption isotherm is described by the Langmuir model, and the maximum adsorption capacity increases with increasing temperature.

A comparative analysis of the sorption materials used for H₂S absorption was carried out during literature analysis:

- an eggshell has a capacity of 2.62 mg/g;²²
- a pure composite based on α -FeOOH—46 mg/g;²³
- a composite based on α -FeOOH with carbon powder—171 mg/g;²⁴
- the coconut shell-activated carbon (ACS-1)—64.27 mg/g;²⁶
- the adsorbent MSM-41—134.38 mg/g.²⁷

Based on the literature data, it can be concluded that mathematical models are used to obtain thermodynamic parameters,²⁸ some of which are universally applicable for sorption processes in both solutions and gases—the Langmuir,²⁹ Freundlich, Temkin, Dubinin–Radushkevich (DR), Redlich–Peterson, Sips, and Toth models.^{30,31} There are also models applicable exclusively to gas sorption—the Guggenheim–Anderson–De Boer model,^{32,33} the classical dual-mode sorption model,³² and Brunauer–Emmett–Teller method.³¹

In the work,³⁴ the process of hydrogen sulfide sorption using activated carbon obtained from nutshells, MWNTs, carbon nanotubes (CNTs) decorated with tungsten nanoparticles (W-CNTs), and amino-functionalized CNTs (F-CNTs) was studied. The sorption isotherms were described by Freundlich, Langmuir, Unilan, Sips, and Toth thermodynamic models. The value of the equilibrium constant by the Freundlich model was 0.3414 for MWNTs, 0.3713 for W-CNTs, and 0.3303 for F-CNTs; by the Langmuir model, the values of equilibrium constants for all sorbents lay in the interval 0.63–0.70; by the Unilan model, the equilibrium constant turned out to be the same in the error range and was \sim 0.50, by the Sips model in the range 0.48–0.51, and for the Toth model, it was 0.24–0.27. The authors of the work made conclusions that the best fit with the experimental data was made by the models Langmuir, Unilan, Sips, and Toth for the MWNT sorbent.

The use of natural materials, having in their composition oxidizing components, looks promising for the purification of gas mixtures, containing substances exhibiting reducing properties. Such natural unique raw materials are ferromanganese ores, the use of which as a sorption material is justified by minimal costs for the preparation and sorption purification of gas emissions. Also attractive is the possibility of using “raw” primary materials, representing unenriched manganese ores, just before the raw material processing procedure to extract the main ore components, which helps to increase the complexity of mineral raw material utilization.

Russia is a world leader in the extraction of manganese ores that can be used as a sorption material with an oxidizing function for the disposal of carbon and sulfur oxides, hydrogen sulfide, and a whole range of volatile organic compounds. Thus, the utilization of process gases of metallurgical works, processing ferromanganese ore, can have a pronounced cyclic nature, which

will significantly reduce the technogenic load on the environment.

Modern production processes are characterized by the introduction of new processes and materials that increase the quality of the target components. The role of theory and the need for thermodynamic and kinetic studies increases the development of new technological schemes and apparatuses. The efficiency of the use of a sorption material is justified by thermodynamic characteristics of processes such as the sorption of hydrogen sulfide by manganese materials which are determined experimentally by further studying the thermodynamic description of the processes and getting values of equilibrium constants and Gibbs energy changes. The obtained thermodynamic characteristics will allow selecting the parameters of sorption units for the purification of gases from toxic impurities.

In the present work, the thermodynamics of the process of hydrogen sulfide sorption by the raw manganese ore of the Ulu-Telyak deposit (Bashkortostan, Russia) and also its basic ore components manganese(IV) oxide and mix of manganese(IV) and iron(III) oxides exhibiting oxidizing properties are investigated. A distinctive feature of the sorption process is the conversion of hydrogen sulfide into elemental sulfur under the action of oxidants; that is, along with chemical interaction, the adsorbate penetration into the sorbent volume can occur, and at reduced pressure and increased temperature, the reverse process—desorption—becomes probable.

To determine the thermodynamic parameters of the hydrogen sulfide sorption process, the equilibrium constant and Gibbs energy change, entropy and enthalpy of the process, sorption isotherms approximated by the mathematical models Langmuir, Freundlich, Temkin, and DR, and equations are presented in Table 1 based on the experimental data.

Table 1. Mathematical Model Description of the Thermodynamic Equilibrium of the Sorption of Hydrogen Sulfide by Manganese Materials

model	non-linear form	linear form
Langmuir	$q = q_{\infty} \frac{K_L \cdot C_{\infty}}{1 + K_L \cdot C_{\infty}}$	$\frac{1}{q} = \frac{1}{q_{\infty}} + \frac{1}{q_{\infty} \cdot K_L}$
Freundlich	$q = K_F \cdot C_{\infty}^{1/\Gamma_{\infty}}$	$\log q = \log K_F + \frac{1}{\Gamma_{\infty}} \cdot \log C_{\infty}$
Temkin	$q = \frac{RT}{K_T} \cdot \ln q_{\infty} C_{\infty}$	$q = \frac{RT}{K_T} \cdot \ln q_{\infty} + \frac{RT}{K_T} \cdot \ln C_{\infty}$
DR	$q = q_{\infty} \cdot e^{-K_{DR} \cdot \varepsilon^2}$	$\ln q = \ln q_{\infty} - K_{DR} \cdot \varepsilon^2$

^a ε —constant of DR: $\varepsilon = RT \cdot \ln\left(1 + \frac{1}{C_{\infty}}\right)$.

METHODOLOGY

The process of hydrogen sulfide sorption was studied on three types of manganese materials. A natural mineral raw material was used from the real manganese ore sample of the Ulu-Telyak deposit, the chemical composition of which is shown in Table 2,³⁵ with a specific surface area of 110 m²/g and an average pore size of 1.36×10^{-8} m. The ore of fractional composition from 1 to 1.6 mm was predried to a constant weight at a temperature of 600 ± 2 °C. The choice of calcination temperature is due to the need to remove physically and chemically bound water included in the hydrated compounds of the natural object.

Table 2. Chemical Composition of Manganese Ore after Heat Treatment

element	mass content, %
MnO	48.24
SiO ₂	24.57
Al ₂ O ₃	8.61
Fe ₂ O ₃	7.50
CaO	7.08
MgO	1.88
K ₂ O	1.54
Na ₂ O	0.20
SO ₃	0.07
P ₂ O ₅	0.07
SrO	0.06
BaO	0.05
V ₂ O ₅	0.04
Cl	0.03
ZnO	0.03
NiO	0.02
SnO ₂	0.01

According to X-ray diffraction analysis, the manganese ore contains a few crystalline phases which are a mixture of iron(II) and (III) oxides FeO–Fe₂O₃, takanelite (Mn,Ca)Mn₄O₉·3H₂O, and quartz SiO₂.³⁵ The basic phases in the ore composition showing oxidizing properties are manganese(IV) oxide and iron(III) oxide, which are chosen as model samples for the comparison of the thermodynamic data of the hydrogen sulfide sorption process on various manganese-containing samples.

A mixture consisting of powdered oxides of manganese(IV) and iron(III) at a mass ratio of 6:1, corresponding to the composition of the ore, was stirred until a homogeneous fraction was obtained. The specific surface area of the oxide mixture was 31 m²/g, while the specific surface area value of manganese(IV) oxide was slightly higher than 75 m²/g.

The sorption process was studied under static conditions from model gas mixtures with the hydrogen sulfide content from 1.25×10^{-3} to 1.28×10^{-4} mol/L at temperatures 253 and 298 K on the samples of the mineral ore, manganese(IV) oxide, and the oxide mixture: MnO₂ and Fe₂O₃.

Hydrogen sulfide was synthesized by a chemical reaction involving the interaction of excess of solid sodium sulfide (chem. part) with orthophosphoric acid with a concentration of 3 M in a Wurtz flask connected through a hose with a tank containing a 6 M NaOH solution used for neutralization of the excess amount of hydrogen sulfide. Aliquots of the obtained gas at the volume from 2 to 26 mL were transferred into a 260 mL chemical tank with 0.050 ± 0.001 g of the manganese material, having previously taken the air from the vessels in the volume equivalent to the introduced H₂S. The contact of phases was carried out for 60 min with constant stirring at a speed of 100 oscillations/min and a given temperature.

The concentration of hydrogen sulfide before and after the sorption process was determined by the chromatographic method using a Thermo Trace GC Ultra gas chromatograph manufactured by Thermo Scientific, USA, using the ratio of the peak areas of the standard samples (125 ppm H₂S, 134 ppm CH₃SH, and 149 ppm C₂H₅SH in a helium atmosphere). The gas mixture was passed through a 6 m long fluoroplastic packing column with an inner diameter of 4 mm filled with a solid carrier “Chromosorb W”. The column temperature was 140 °C, that of the evaporator was 140 °C, that of the flame photometric

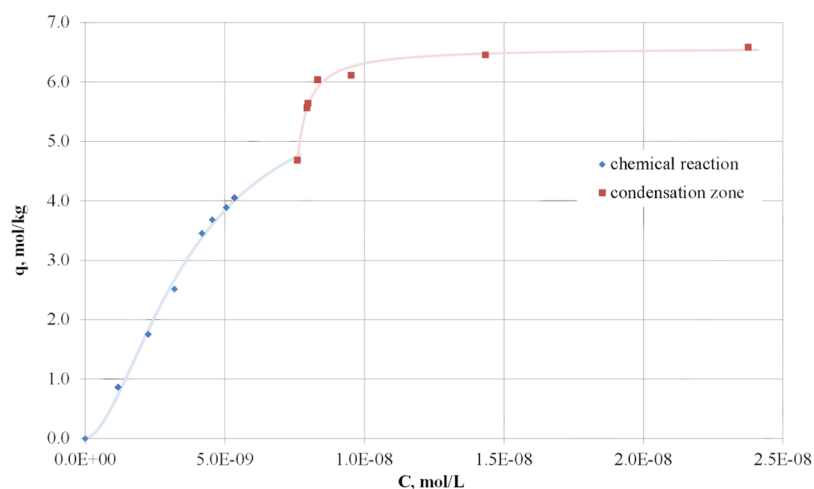


Figure 1. Isotherm of hydrogen sulfide sorption on the manganese ore at 253 K. Two areas are clearly defined on the sorption isotherm, the first of which corresponds to the process taking place due to the chemical reaction and the second—due to the condensation of hydrogen sulfide, which is a zone of physical sorption.

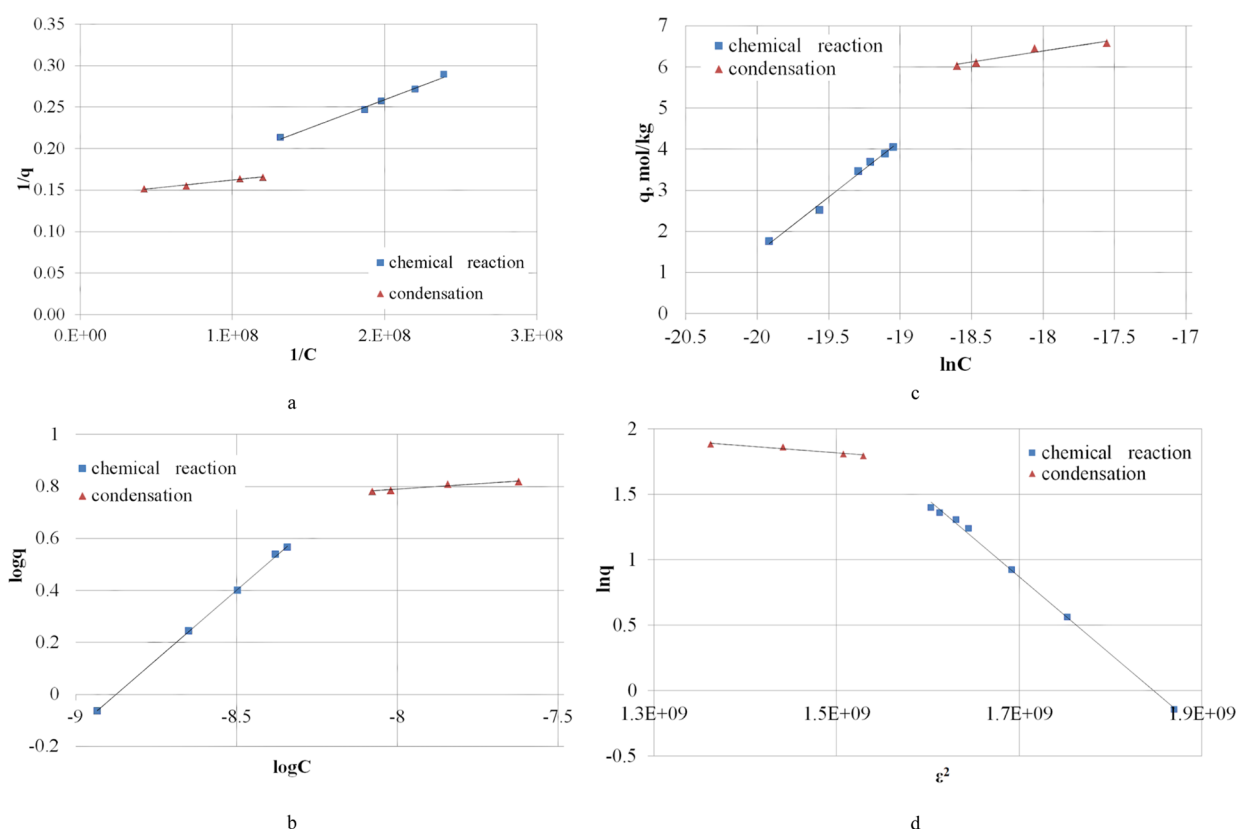


Figure 2. Linear forms of the hydrogen sulfide sorption isotherm on the manganese ore at a temperature of 253 K using models of thermodynamic description: (a) Langmuir; (b) Freundlich; (c) Temkin; (d) DR.

detector was 180 °C, and pressure was 45 Pa. The air flow rate was 120 mL/min, and the hydrogen flow rate was 90 mL/min.

RESULTS AND DISCUSSION

The value of the capacity of the sorption materials was calculated by the formula

$$q = \frac{(C_0 - C_\infty) \cdot V}{m} \quad (1)$$

where C_0 and C_∞ are the initial and equilibrium concentration of hydrogen sulfide in the gas mixture, mol/L; V is the volume of the gas mixture, mL; and m is the mass of the sorbent, g.

The isotherm of hydrogen sulfide sorption on the manganese ore at a temperature of 253 K is presented in Figure 1.

To obtain the thermodynamic parameters of the process, a mathematical description was studied and linear forms of the isotherm of hydrogen sulfide sorption on the mineral ore were built (Figure 2).

Using the approximation equations of the linear forms of sorption isotherms, the values of equilibrium constants K and

Table 3. Thermodynamic Description of Hydrogen Sulfide Sorption by the Manganese Ore at 253 K

model	process	equation of approximation	correlation coefficient R^2	K	ΔG_{253} , kJ/mol
Langmuir	chemical reaction	$y = 7 \times 10^{-10}x + 0.1202$	0.9915	$(1.72 \pm 0.09) \times 10^8$	-39.88 ± 1.99
	condensation	$y = 2 \times 10^{-10}x + 0.1$	0.9789	$(7.16 \pm 0.36) \times 10^8$	-42.89 ± 2.14
Freundlich	chemical reaction	$y = 1.0735x + 9.5264$	0.9897	$(3.36 \pm 0.17) \times 10^9$	-46.14 ± 2.31
	condensation	$y = 0.0861x + 1.4784$	0.9364	30.09 ± 1.50	-7.16 ± 0.36
Temkin	chemical reaction	$y = 2.73x + 56.065$	0.9926	770.12 ± 38.51	-13.98 ± 0.70
	condensation	$y = 0.5436x + 16.174$	0.9397	3867.60 ± 193.38	-17.38 ± 0.87
DR	chemical reaction	$y = -6 \times 10^{-9}x + 10.918$	0.9973	$(6.00 \pm 0.30) \times 10^{-9}$	39.80 ± 1.99
	condensation	$y = -5 \times 10^{-10}x + 2.6277$	0.9399	$(5.00 \pm 0.25) \times 10^{-10}$	45.03 ± 2.25

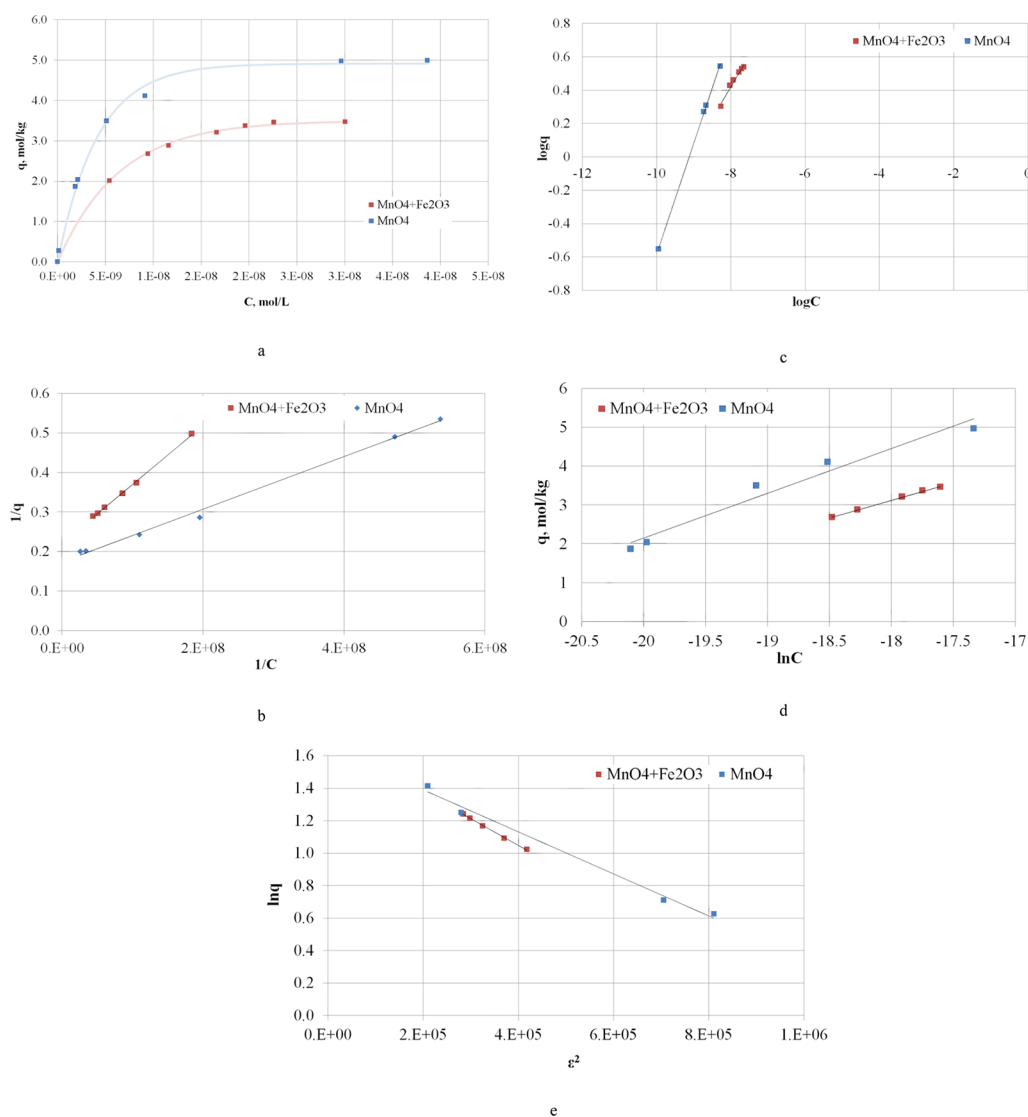


Figure 3. Sorption isotherms of hydrogen sulfide $\text{MnO}_4 + \text{Fe}_2\text{O}_3$ and MnO_4 (a) at 253 K and linear forms of isotherms using Langmuir (b), Freundlich (c), Temkin (d), and DR (e) models.

changes in the Gibbs energy of the two processes ΔG_{253} accompanying the sorption of H_2S were calculated (Table 3).

A comparative analysis of the data obtained using the four thermodynamic models shows an unsatisfactory interpretation of the H_2S sorption process based on the DR model. According to the obtained results, the sorption process is characterized by a positive value of Gibbs energy, which contradicts the experimental fact—spontaneous course of the process with the formation of the reaction products: $2\text{MnO}_2(\text{s}) + \text{H}_2\text{S}(\text{g}) = \text{S}(\text{s}) + \text{Mn}_2\text{O}_3(\text{s}) + \text{H}_2\text{O}(\text{g})$,³⁴ identified by X-ray phase analysis using a

Shimadzu XRD-7000 X-ray diffractometer manufactured by Shimadzu Corporation, Japan.

High correlation coefficients were obtained by approximating the experimental dependence by the Langmuir, Freundlich, and Temkin models.

However, the values of the Gibbs constant and energy of hydrogen sulfide oxidation by manganese oxide calculated using the Temkin model are 770.12 ± 38.51 and -13.98 ± 0.70 kJ/mol, which are significantly lower than the calculated standard

Table 4. Thermodynamic Description of Hydrogen Sulfide Sorption by the Mixture of Manganese(IV) and Iron(III) Oxides and Manganese(IV) Oxide at a Temperature of 253 K

material	model	equation of approximation	R ²	K	ΔG ₂₅₃ , kJ/mol
MnO ₄ + Fe ₂ O ₃	Langmuir	$y = 1 \times 10^{-9}x + 0.2204$	0.9985	$(2.20 \pm 0.11) \times 10^8$	-40.41 ± 2.02
	Freundlich	$y = 0.3758x + 3.4271$	0.9729	2673.62 ± 133.68	-16.60 ± 0.83
	Temkin	$y = 0.9081x + 19.469$	0.9977	2315.20 ± 115.76	-16.30 ± 0.81
	DR	$y = -2 \times 10^{-6}x + 1.7129$	0.9978	$(2.00 \pm 0.01) \times 10^{-7}$	27.59 ± 1.38
MnO ₄	Langmuir	$y = 7 \times 10^{-10}x + 0.1736$	0.9959	$(2.48 \pm 0.12) \times 10^8$	-40.66 ± 2.03
	Freundlich	$y = 0.6681x + 6.0955$	0.9995	$(1.25 \pm 0.06) \times 10^6$	-29.526 ± 1.48
	Temkin	$y = 1.1524x + 25.196$	0.9637	1824.39 ± 91.22	-17.79 ± 0.79
	DR	$y = -1 \times 10^{-6}x + 1.6487$	0.9915	$(1.00 \pm 0.05) \times 10^{-8}$	29.05 ± 1.45

values of thermodynamic characteristics at 253 K: 6.58×10^{28} and -140.46 ± 7.02 kJ/mol.

The most reliable results are the Gibbs constant and energy values calculated using the Langmuir models: $(1.72 \pm 0.09) \times 10^8$, -39.88 ± 1.99 kJ/mol and Freundlich $(3.36 \pm 0.17) \times 10^9$, -46.14 ± 2.31 kJ/mol.

However, the interpreted results of the hydrogen sulfide condensation stage using the Freundlich model are characterized by lower values of the correlation coefficient (0.94). The Langmuir model describes the condensation process more reliably; the correlation coefficient is 0.98.

High values of equilibrium constants of hydrogen sulfide sorption processes, actually, both as a chemical reaction and sorption, characterize the shift of the equilibrium toward the reaction products, and as a consequence, the degree of irreversibility of the process.

Real sorption materials have a heterogeneous surface; the molecules adsorbed on this surface interact both with the material components and with each other. The effect of the interaction of adsorbed particles manifests itself as a change in both the free energy and the heat of chemisorption depending on the degree of surface coverage by the adsorbed substance. Therefore, the absence of precise data on the nature of the interaction of adsorbed particles makes it difficult to use the known equations to derive sorption isotherms.

An equivalent form of the hydrogen sulfide sorption isotherm on manganese(IV) and iron(III) oxides should be expected. The sorption of hydrogen sulfide by a mixture of oxides MnO₄ + Fe₂O₃ and individual oxide MnO₄ was studied at 253 K; the mathematical description was studied using the same four models. Figure 3 shows the sorption isotherms and their linear forms.

In contrast to the isotherm of H₂S sorption by the ore on the experimental dependence of the sorption value on the equilibrium gas concentration, only one dependence, which corresponds to chemical reaction, is observed.³⁵

The thermodynamic description of hydrogen sulfide sorption by the mixture of manganese(IV) and iron(III) oxides is presented in Table 4.

Adequate values of the equilibrium constant at $R^2 = 0.99$, which satisfactorily converge with the chemical reaction constant on the ore surface, have been obtained using the Langmuir model (MnO₄ + Fe₂O₃, $K = (2.20 \pm 0.11) \times 10^8$ and MnO₄, $K = (2.48 \pm 0.12) \times 10^8$), the applicability of which is explained by the absence of physical polymolecular adsorption.

The morphology of the ore samples before hydrogen sulfide sorption and after at 253 K was analyzed with a TESCAN firm Vega 3 scanning electron microscope. The electron microscopic images of the sample particles were obtained in the secondary electron scanning resolution mode. The analyzed powdered

samples were applied onto a conductive tape and shot at 10 kV (Figure 4), the accelerating voltage was 10 kV, and the emission current was 120 μA.

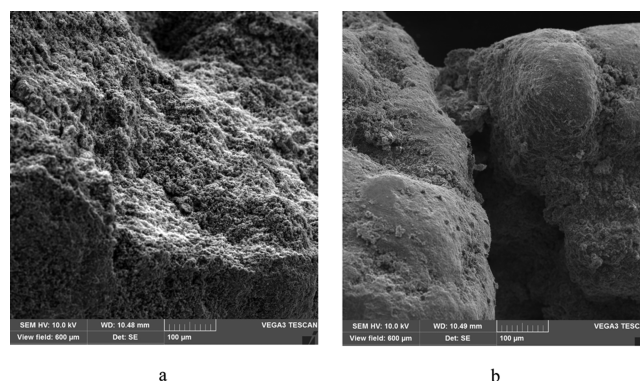


Figure 4. Surface images before the (a) hydrogen sulfide sorption process and after (b) on the manganese ore at 253 K.

According to the results of morphological analysis, a change in the surface of the sample of the “raw” manganese ore, where elemental sulfur, formed in the process of hydrogen sulfide sorption by the oxidation of manganese(IV) oxide, is clearly visible.

To determine the thermal effect of the hydrogen sulfide sorption process on manganese materials, isotherms at 298 K were obtained and interpreted by the Langmuir model (Figure 5 and Table 5).

Using isobar equations, we calculated the enthalpy of the hydrogen sulfide sorption process on the samples of the studied materials in the temperature range of 253–298 K

$$\Delta H_{(T_2-T_1)} = R \cdot \frac{T_1 \cdot T_2}{T_2 - T_1} \cdot \ln \frac{K_2}{K_1} \quad (2)$$

where K_1 and K_2 are chemisorption equilibrium constants at the respective temperatures T_1 and T_2 , and the entropy value is given by formula 3

$$\Delta S_T = \frac{1}{T} \cdot (\Delta H_T - \Delta G_T) \quad (3)$$

The results of a thermodynamic calculation based on the values of the constants of the chemisorption equilibrium in comparison with the values of thermal effects of the H₂S sorption process, measured using a thermochemical gas analyzer IKA C2000 basic [IKA WERKE (Germany)], are given in Table 6.³⁵

The capacity values of the manganese samples at different temperatures are given in Table 7.

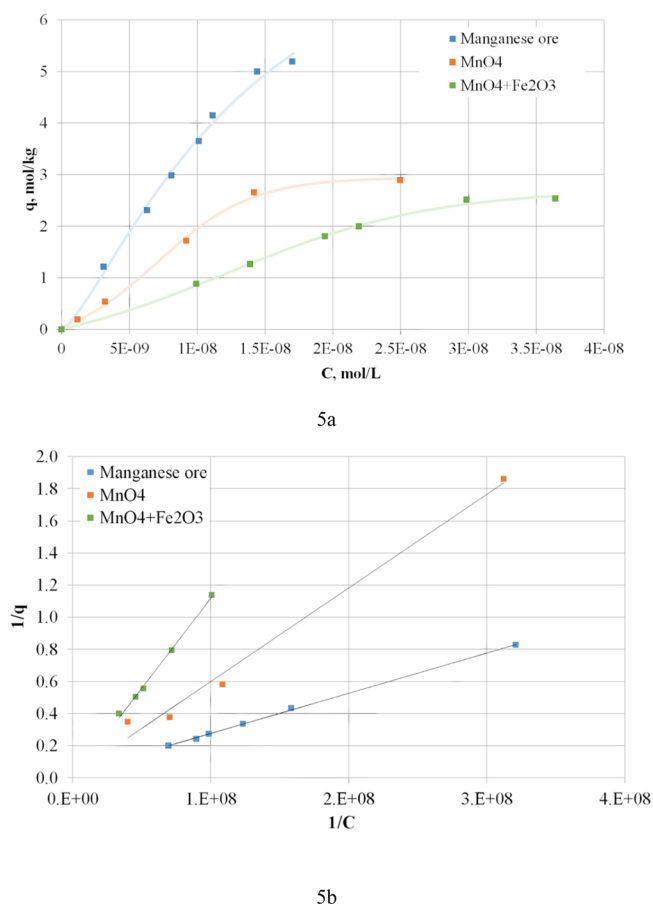


Figure 5. Isotherms of hydrogen sulfide sorption by the ore, MnO₄ + Fe₂O₃, and MnO₄ (a) at a temperature of 298 K and linear forms of Langmuir isotherms (b).

With increasing temperature, a decrease in the sorption characteristics of the materials is observed following a decrease in the reaction yield. The manganese ore has a higher value of limiting capacity compared with oxides, which is explained by the presence of crystalline and amorphous phases of silicates and hydrated silicon oxide in it. The phases in ore composition, indifferent to the oxidation of hydrogen sulfide to elementary sulfur, provide a sorption effect. The heating of the samples of the ore is accompanied by the evolution of hydrogen sulfide in a gas phase, whereas from a surface of oxides, the evolution of H₂S was not observed. Thus, only a chemical reaction takes place on the surface of the oxides. A satisfactory agreement of the constants of chemical equilibrium on all samples during the sorption of hydrogen sulfide characterizes the same oxidation–reduction reaction; iron(III) oxide in the ore and the oxide mixture show only catalytic activity.³⁵ Also, the lower value of the limiting capacity and specific surface of the oxide mixture in comparison with manganese oxide is explained just by the presence of Fe₂O₃ in the sample.

The calculated enthalpy values from the temperature dependence of the chemical equilibrium constants correspond to the value of the heat effect measured directly during the hydrogen sulfide chemisorption process accompanied by a decrease in the entropy factor.

The effect of the interaction of adsorbed particles depending on the degree of surface coverage by the adsorbed substance manifests itself in the changes in the free energy, heat, and entropy of chemisorption, the evaluation of which allows a reliable interpretation of the surface activity of sorbents, including those exhibiting catalytic activity.

CONCLUSIONS

In this work, studies were carried out on the sorption of hydrogen sulfide on the raw manganese ore, a mixture of manganese(IV) oxide and iron(III) oxide at a ratio of 6:1, and on pure manganese(IV) oxide at the temperatures of 253 and 298 K.

The thermodynamic characteristics of the obtained hydrogen sulfide sorption isotherms on manganese materials at 253 K were described using Langmuir, Freundlich, Temkin, and DR models. The most reliable results are the values of the Gibbs constant and energy calculated using the Langmuir model on the ore: $(1.72 \pm 0.09) \times 10^8$, -39.88 ± 1.99 kJ/mol; MnO₄ + Fe₂O₃: $K = (2.20 \pm 0.11) \times 10^8$, -40.41 ± 2.02 kJ/mol; and MnO₄: $K = (2.48 \pm 0.12) \times 10^8$, -40.66 ± 2.03 kJ/mol.

High values of the equilibrium constants of hydrogen sulfide sorption processes, actually, both as a chemical reaction and sorption, characterize the shift of the equilibrium toward the reaction products, and as a consequence, the degree of irreversibility of the process.

According to the results of morphological analysis, a change in the surface of the “raw” manganese ore sample is clearly visible, on which elemental sulfur, formed during the sorption of hydrogen sulfide by the oxidation of manganese oxide(IV), is identified.

The manganese ore has a higher limiting capacity value of 6.58 ± 0.33 mol/kg compared to the oxides— 3.47 ± 0.17 mol/kg for MnO₄ + Fe₂O₃ and 5.00 ± 0.25 mol/kg for MnO₄—that is explained by the presence of crystalline and amorphous silicate and hydrated silicon oxide phases in it. The phases in the ore composition, indifferent to the oxidation of hydrogen sulfide to elementary sulfur, provide a sorption effect. The heating of the ore samples is accompanied by the evolution of hydrogen sulfide in a gas phase, whereas from a surface of oxides, the evolution of H₂S was not observed. Thus, only a chemical reaction takes place on the surface of the oxides.

The calculated enthalpy values from the temperature dependence of the chemical equilibrium constants for the ore: -68.98 ± 3.45 kJ/mol, MnO₄: + Fe₂O₃ -244.03 ± 12.20 kJ/mol, and MnO₄: -103.826 ± 5.19 kJ/mol correspond to the magnitude of the heat effect measured directly during the chemisorption process hydrogen sulfide, accompanied by a decrease in the entropy factor.

Table 5. Thermodynamic Description of Hydrogen Sulfide Sorption by the Manganese Ore, Oxides MnO₄ + Fe₂O₃, and MnO₄ at 298 K

material	equation of approximation	R ²	K	ΔG ₂₉₈ , kJ/mol
manganese ore	$y = 3 \times 10^{-9}x + 0.0264$	0.9992	$(8.80 \pm 0.44) \times 10^6$	-39.69 ± 1.98
MnO ₄ + Fe ₂ O ₃	$y = 1 \times 10^{-8}x + 6 \times 10^{-5}$	0.9964	$(6.00 \pm 0.30) \times 10^3$	-21.54 ± 1.08
MnO ₄	$y = 6 \times 10^{-9}x + 0.017$	0.9891	$(2.83 \pm 0.14) \times 10^6$	-36.79 ± 1.84

Table 6. Thermodynamic Parameters of Hydrogen Sulfide Sorption by Manganese Materials

material	T, K	K	$-\Delta G_T$, kJ/mol	$-\Delta H_{253}$, kJ/mol ³⁵	$-\Delta S_{253}$, J/mol·K	$-\Delta H_{(253-298)}$, kJ/mol	$-\Delta S_{253}$, J/mol·K
manganese ore	253	$(1.72 \pm 0.09) \times 10^8$	39.88 ± 1.99	69.44 ± 1.39	116.82 ± 5.84	68.98 ± 3.45	114.99 ± 5.75
	298	$(8.80 \pm 0.44) \times 10^6$	39.69 ± 1.98				
MnO ₄ + Fe ₂ O ₃	253	$(2.20 \pm 0.11) \times 10^8$	40.41 ± 2.02	226.11 ± 11.31	734.01 ± 11.31	244.03 ± 12.20	804.83 ± 40.24
	298	$(6.00 \pm 0.30) \times 10^3$	21.54 ± 1.08				
MnO ₄	253	$(2.48 \pm 0.12) \times 10^8$	40.66 ± 2.03	100.46 ± 5.02	236.37 ± 11.82	103.826 ± 5.19	249.66 ± 12.48
	298	$(2.83 \pm 0.14) \times 10^6$	36.79 ± 1.84				

Table 7. Value of Limiting Capacity for the Manganese Materials at the Temperatures of 253 and 298 K

material	T, K	q, mol/kg
manganese ore	253	6.58 ± 0.33
	298	5.19 ± 0.33
MnO ₄ + Fe ₂ O ₃	253	3.47 ± 0.17
	298	2.54 ± 0.13
MnO ₄	253	5.00 ± 0.25
	298	2.89 ± 0.14

AUTHOR INFORMATION

Corresponding Author

Maria A. Ponomareva – Saint Petersburg Mining University, St Petersburg 199106, Russia; orcid.org/0000-0002-7790-8178; Email: mashulka-05@mail.ru

Authors

Olga V. Cheremisina – Saint Petersburg Mining University, St Petersburg 199106, Russia; orcid.org/0000-0002-3045-3313

Victor A. Bolotov – Saint Petersburg Mining University, St Petersburg 199106, Russia; orcid.org/0000-0001-8114-1689

Artyom S. Osipov – Saint Petersburg Mining University, St Petersburg 199106, Russia; orcid.org/0000-0002-5192-9085

Alexandr V. Sitko – Saint Petersburg Mining University, St Petersburg 199106, Russia; orcid.org/0000-0003-1685-0731

Complete contact information is available at:

<https://pubs.acs.org/10.1021/acsomega.1c06037>

Author Contributions

The manuscript was written through the contributions of all authors. All authors have given approval to the final version of the manuscript. O.V.C., M.A.P., V.A.B., A.S.O., and A.V.S. contributed equally.

Notes

The authors declare no competing financial interest.

ACKNOWLEDGMENTS

This research was carried out at the expense of the grant for the state assignment in the sphere of scientific activity for 2021 no. FSRW-2020-0014. The author's team is grateful to the Scientific Center "Problems of mineral and technogenic resources processing" of St. Petersburg Mining University, on the basis of which the research was carried out.

REFERENCES

(1) Glazev, M.; Bazhin, V. Environmental technologies in the production of metallurgical silicon. *Scientific and Practical Studies of Raw Material Issues—Proceedings of the Russian—German Raw*

Materials Dialogue: A Collection of Young Scientists Papers and Discussion; CRC Press, 2020; pp 114–119.

(2) Dubovikov, O. A.; Brichkin, V. N.; Brichkin, V. N.; Ris, A. D.; Sundurov, A. V. Thermochemical activation of hydrated aluminosilicates and its importance for alumina production. *Non-ferrous Metals* **2018**, *45*, 10–15.

(3) Taranina, O. A.; Burkat, V. S.; Volkodaeva, M. V. Analysis of the Concentration of Gas-Phase and Solid-Phase Polyaromatic Hydrocarbons in Industrial Emissions from Aluminum Production. *Metalurgist* **2020**, *63*, 1227–1236.

(4) Lebedev, A. B.; Utkov, V. A.; Utkov, V. A.; Khalifa, A. A. Sintered Sorbent Utilization for H₂S Removal from Industrial Flue Gas in the Process of Smelter Slag Granulation. *J. Min. Inst.* **2019**, *237*, 292–297.

(5) Shcherbakova, N.; Khaikin, M. City as an Object of Ecological and Economic Researches: The Example of Russian Cities. *IOP Conf. Ser.: Mater. Sci. Eng.* **2019**, *272*, 032119.

(6) Ivanik, S.; Ilyukhin, D. Flotation extraction of elemental sulfur from gold-bearing cakes. *J. Min. Inst.* **2020**, *242*, 202–208.

(7) Pashkevich, M. A.; Petrova, T. A. Assessment of widespread air pollution in the megacity using geographic information systems. *J. Min. Inst.* **2017**, *228*, 738–742.

(8) Povarov, V. G.; Kopylova, T. N.; Sinyakova, M. A.; Rudko, V. A. Quantitative Determination of Trace Heavy Metals and Selected Rock-Forming Elements in Porous Carbon Materials by the X-ray Fluorescence Method. *ACS Omega* **2021**, *6*, 24595–24601.

(9) Kovshov, S. V.; Skamyin, A. N. Treatment of agricultural wastes with biogas-vermiculture. *Environ. Earth Sci.* **2017**, *76*, 660.

(10) Sulimova, M. A. About the interchangeability of iron-manganese nodules of the Pacific and the Baltic Sea. *IOP Conf. Ser.: Mater. Sci. Eng.* **2020**, *919*, 062039.

(11) Meng, X. M.; De Jong, W.; Verkooijen, A. H. M. Thermodynamic Analysis and Kinetics Model of H₂S Sorption Using Different Sorbents. *Environ. Prog. Sustainable Energy* **2009**, *28*, 360–371.

(12) Moon, D. J.; Lim, W. T.; Seff, K. Crystal structure of a hydrogen sulfide sorption complex of anhydrous Mn²⁺-exchanged zeolite Y (FAU, Si/Al = 1.56). *Microporous Mesoporous Mater.* **2019**, *279*, 432–438.

(13) Sarwar, A.; Ali, M.; Khoja, A. H.; Nawar, A.; Waqas, A.; Liaquat, R.; Naqvi, S. R.; Asjid, M. Synthesis and characterization of biomass-derived surface-modified activated carbon for enhanced CO₂ adsorption. *J. CO₂ Util.* **2021**, *46*, 101476.

(14) Orojlou, S. H.; Zargar, B.; Rastegarzadeh, S. Metal oxide/TiO₂ nanocomposites as efficient adsorbents for relatively high temperature H₂S removal. *J. Nat. Gas Sci. Eng.* **2018**, *59*, 363–373.

(15) Lin, Y.-H.; Chen, Y.-C.; Chu, H. The mechanism of coal gas desulfurization by iron oxide sorbents. *Chemosphere* **2015**, *121*, 62–67.

(16) Quan, W.; Wang, X.; Song, C. Selective Removal of H₂S from Biogas Using Solid Amine-Based «Molecular Basket» Sorbent. *Energy Fuels* **2017**, *31*, 9517–9528.

(17) Okonkwo, C. N.; Fang, H.; Sholl, D. S.; Leisen, J. E.; Jones, C. W. Effect of Humidity on the Sorption of H₂S from Multicomponent Acid Gas Streams on Silica-Supported Sterically Hindered and Unhindered Amines. *ACS Sustainable Chem. Eng.* **2020**, *8*, 10102–10114.

(18) Fenouil, A.; Lynn, S. Study of Calcium-Based Sorbents for High-Temperature H₂S Removal. 2. Kinetics of H₂S Sorption by Calcined Limestone. *Ind. Eng. Chem. Res.* **1995**, *34*, 2334–2342.

(19) Wjilhi, S.; Aouaini, F.; Erto, A.; Balsamo, M.; Lamine, A. B. Advanced interpretation of CO₂ adsorption thermodynamics onto

porous solids by statistical physics formalism. *Chem. Eng. J.* **2021**, *406*, 126669.

(20) Yoosuk, B.; Methakhup, P.; Prasassarakich, P. Binary sorption of CO₂ and H₂S over polyamine modified fumed silica pellets in a double stage fixed-bed system. *Process Saf. Environ. Prot.* **2017**, *106*, 173–179.

(21) Bartik, A.; Benedikt, F.; Lunzer, A.; Walcher, C.; Müller, S.; Hofbauer, H. Thermodynamic investigation of SNG production based on dual fluidized bed gasification of biogenic residues. *Biomass Convers. Biorefin.* **2021**, *11*, 95–110.

(22) Ahmad, W.; Sethupathi, S.; Munusamy, Y.; Kanthasamy, R. Valorization of raw and calcined chicken eggshell for sulfur dioxide and hydrogen sulfide removal at low temperature. *Catalysts* **2021**, *11*, 295.

(23) Lee, S.; Lee, T.; Kim, D. Adsorption of Hydrogen Sulfide from Gas Streams Using the Amorphous Composite of α -FeOOH and Activated Carbon Powder. *Ind. Eng. Chem. Res.* **2017**, *56*, 3116–3122.

(24) Wang, J.; Liang, B.; Parnas, R. Manganese-based regenerable sorbents for high temperature H₂S removal. *Fuel* **2013**, *107*, 539–546.

(25) Daneshyar, A.; Ghaedi, M.; Sabzehmeidani, M. M.; Daneshyar, A. H₂S adsorption onto Cu-Zn-Ni nanoparticles loaded activated carbon and Ni-Co nanoparticles loaded γ -Al₂O₃: Optimization and adsorption isotherms. *J. Colloid Interface Sci.* **2017**, *490*, 553–561.

(26) Shi, L.; Yang, K.; Zhao, Q.; Wang, H.; Cui, Q. Characterization and Mechanisms of H₂S and SO₂ Adsorption by Activated Carbon. *Energy Fuels* **2015**, *29*, 6678–6685.

(27) Zhang, J. J.; Wang, W. Y.; Wang, G. J.; Kai, C.; Song, H.; Wang, L. Equilibrium, Kinetic and Thermodynamic Studies on Adsorptive Removal of H₂S from Natural Gas by Amine Functionalisation of MCM-41. *Prog. React. Kinet. Mech.* **2017**, *42*, 221–234.

(28) Hassanpouryouzband, A.; Farahani, M. V.; Yang, J.; Tohidi, B.; Chuvilin, E.; Istomin, V.; Bukhanov, B. Solubility of Flue Gas or Carbon Dioxide-Nitrogen Gas Mixtures in Water and Aqueous Solutions of Salts: Experimental Measurement and Thermodynamic Modeling. *Ind. Eng. Chem. Res.* **2019**, *58*, 3377–3394.

(29) Yang, Y.; Liu, S.; Zhao, W.; Wang, L. Intrinsic relationship between Langmuir sorption volume and pressure for coal: Experimental and thermodynamic modeling study. *Fuel* **2019**, *241*, 105–117.

(30) Georgiadis, A. G.; Charisiou, N. D.; Gaber, S.; Polychronopoulou, K.; Yentekakis, I. V.; Goula, M. A. Adsorption of Hydrogen Sulfide at Low Temperatures Using an Industrial Molecular Sieve: An Experimental and Theoretical Study. *ACS Omega* **2021**, *6*, 14774–14787.

(31) Laskar, I. I.; Hashisho, Z. Insights into modeling adsorption equilibria of single and multicomponent systems of organic and water vapors. *Sep. Purif. Technol.* **2020**, *241*, 116681.

(32) Vopička, O.; Friess, K. Analysis of Gas Sorption in Glassy Polymers with the GAB Model: An Alternative to the Dual Mode Sorption Model. *J. Polym. Sci., Part B: Polym. Phys.* **2014**, *52*, 1490–1495.

(33) Lanč, M.; Pilnáček, K.; Mason, C. R.; Budd, P. M.; Rogan, Y.; Malpass-Evans, R.; Carta, M.; Comesañ, B.; Neil, G.; Keown, B. M.; Jansen, J. C.; Vopička, O.; Friess, K. Gas sorption in polymers of intrinsic microporosity: The difference between solubility coefficients determined via time-lag and direct sorption experiments. *J. Membr. Sci.* **2019**, *570–571*, 522–536.

(34) Mohamadizadeh, A.; Towfighi, J.; Rashidi, A.; Mohajeri, A.; Golkar, M. Modification of Carbon Nanotubes for H₂S Sorption. *Ind. Eng. Chem. Res.* **2011**, *50*, 8050–8057.

(35) Cheremisina, E.; Cheremisina, O.; Ponomareva, M.; Bolotov, V.; Fedorov, A. Kinetic features of the hydrogen sulfide sorption on the ferro-manganese material. *Metals* **2021**, *11*, 90.